

COMPLEXATION STATE OF IRON AND COPPER IN AMBIENT PARTICULATE
MATTER AND ITS EFFECT ON THE OXIDATIVE POTENTIAL

BY

JINLAI WEI

THESIS

Submitted in partial fulfillment of the requirements
for the degree of Master of Science in Environmental Engineering in Civil Engineering
in the Graduate College of the
University of Illinois at Urbana-Champaign, 2018

Urbana, Illinois

Adviser:

Assistant Professor Vishal Verma

ABSTRACT

Transition metals have long been recognized as an important component contributing to the toxicological property of ambient particulate matter (PM). Various methods of assessing this toxicity have been applied, including measuring the capability of PM components to generate reactive oxygen species (ROS), and the capability of consuming antioxidants. However, whether transition metals are complexed with organic compounds or free in ambient PM, which could be an important factor determining their ability to generate ROS, is not well understood. We target to investigate the complexation states of important atmospheric metals in this study. A novel fractionation scheme is developed to separate Fe and Cu from ambient PM into hydrophilic, hydrophobic and inorganic fractions. The scheme has been validated by applying it on a mixture of Suwannee River fulvic acid (SRFA) and Fe or Cu. SRFA is selected as a model compound as it represents the humic-like substances present in ambient PM, which are believed to be complexed with Fe and Cu. The results show that a significant amount of iron pre-mixed with SRFA is detected in both hydrophobic and hydrophilic fractions, indicating potential complexation with both types of organic substances. Similar tests conducted with the ambient PM show up to 70-80% of iron complexed with organic compounds. Fe and SRFA show strong synergistic effect in the generation of hydroxyl radical in different antioxidants systems (surrogate lung fluid, ascorbic acid and dithiothreitol), which is attributed to the higher efficiency of Fe-SRFA complexes to convert H_2O_2 to $\cdot\text{OH}$ (Fenton reaction) than Fe alone. Although, Cu and SRFA show additive effect in $\cdot\text{OH}$ production, while they are antagonistic in the consumption of antioxidants (ascorbic acid and glutathione). Overall, the organic complexation of metals in ambient PM could significantly alter the oxidative potential of ambient PM and needs to be accounted for apportioning the contribution of metals in aerosol toxicity.

TABLE OF CONTENTS

CHAPTER 1: INTRODUCTION.....	1
CHAPTER 2: MATERIAL AND METHODS.....	5
CHAPTER 3: RESULTS AND DISCUSSION.....	14
CHAPTER 4: CONCLUSION.....	28
REFERENCES.....	29
APPENDIX A: SUPPLEMENTARY INFORMATION.....	39

CHAPTER 1: INTRODUCTION

Numerous epidemiological studies have linked ambient particulate matter (PM) to adverse health outcomes upon inhalation.¹⁻³ PM-borne transition metals, which are dominated by Fe and Cu,^{4,5} are recognized as one of the most important components to induce toxicological effects, including acute airway inflammation,^{6,7} cardiopulmonary illnesses,^{8,9} and atherosclerosis.¹⁰ Oxidative potential (OP) of ambient particles has been widely accepted as an indicator of PM-induced toxicity.¹¹⁻¹³ Assessing OP with acellular assays has identified the significant contribution of Fe and Cu through the generation of reactive oxygen species (ROS).¹⁴⁻¹⁷

Traditionally, the OP of transition metals was assessed using pure metal compounds (i.e. inorganic solution). However, ambient transition metals are efficient in forming complexes with organic compounds and seldom exist in free form. The chelation of transition metals (primarily Fe and Cu) in the atmosphere has been studied due to its impact on mobility,¹⁸ bioavailability¹⁹ and redox activity^{20,21} of trace metals. Paris et al.²² identified oxalate, malonate, tartrate and humic acid as important organic species to complex iron in rainwater, thus enhancing the Fe solubility and stabilizing Fe in dissolved form after wet deposition in seawater. Scheinhardt et al.²³ investigated complexation of trace metals in size-segregated aerosol particles, and indicated that malate, malonate and oxalate are important complexing agents of Cu²⁺ in most of the stages from 0.05-10 μm . Humic and fulvic acids were also found in strong complexes associated with copper in rainwater samples²⁴, potentially affecting the redox cycling of copper both in vivo²⁵ and in vitro.²⁶ Despite the importance of metal-organic chelation, the extent of metal complexation in ambient PM is not well understood. Visual MINTEQ is a frequently used model to study the speciation of metal-organic complexes.²⁷⁻²⁹ However, to provide the equilibrium concentrations of the resulting substances, it requires the stability constants of all potentially present complexes.²³ In light of our

limited understanding of organic aerosols in terms of their chemical composition,^{30,31} it could be rather challenging to make a thorough characterization of PM-borne metal-organic complexes using Visual MINTEQ.

A number of studies have investigated the impact of metal-organic complexes on the oxidizing power of these metals, both in natural water^{32,33} and in ambient aerosols.³⁴ Well known for their similarity of chemical composition and properties to some organic aerosols, humic acid (HA) and fulvic acid (FA) are underlined due to their notable ability of metal-binding and their role in redox cycling of transition metals.^{35,36} Currently, the generation of ROS, especially hydroxyl radical, has been widely accepted for the assessment of PM-induced toxicity.^{15,16,37} The $\cdot\text{OH}$ production catalyzed by Fe or Cu is a net reaction consisting of the reduction from dissolved oxygen to O_2^- , the conversion from O_2^- to H_2O_2 , and the destruction of H_2O_2 to generate $\cdot\text{OH}$, known as Fenton reaction or Fenton-like reaction:³⁸

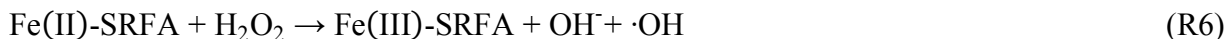


And Fe(III) can be cycled back to its reduced form by antioxidants (AO, e.g. dithiothreitol (DTT) and ascorbate):¹²



The presence of Fe(II)-organic ligands has been proved to be capable to expedite $\cdot\text{OH}$ generation in this process. Voelker et al.³⁹ concluded that Fe(II)-fulvate complexes could convert H_2O_2 to $\cdot\text{OH}$ more efficiently than Fe(II)-aquo complexes at pH 5. Suwannee river fulvic acid (SRFA) is a commonly chosen proxy of water-soluble atmospheric humic-like substances (HULIS).^{40,41} Under

physiological pH, it is also hypothesized^{42,43} that Fe(II)-SRFA complexes enhance the reaction rate of R1 and R3, thus facilitating ·OH production:



However, as SRFA demonstrates noticeable response in DTT consumption,⁴⁴ an alternative explanation for the Fe-SRFA synergy is the enhanced conversion of H₂O₂ formed in the SRFA-DTT system by Fe. The confounding of the positive interaction of Fe-SRFA complexes depends on the competition between two proposed mechanisms. Additionally, fewer studies have discussed the effect of Cu-SRFA complexes on Cu(II)'s oxidizing power, despite that Cu(II) is more prone to be bound by HULIS than Fe(II).⁴⁵ Fulda et al.⁴⁶ and Maurer et al.⁴⁷ studied the complexation and reduction of Cu(II) by soil humic acid, but it has not been confirmed if the Cu(II)-SRFA complexation would exert influence on copper's redox activity. Apparently, the Fe(II)-SRFA and Cu(II)-SRFA complexes need to be better understood to elucidate their potential impact on the oxidative stress of ambient Fe(II) and Cu(II).

In this study, A novel scheme was developed to fractionate iron and copper in ambient samples using C18 solid phase extraction (SPE) column (60A, 40-63µm, Endcapped, 100g). C18 separation method has been conventionally used to extract atmospheric HULIS; some studies focused on the chemical composition of HULIS^{48,49}, while others focused on its oxidative potential^{50,51}. However, few studies have recognized C18 column for its ability to fractionate transition metals in aerosol particles. Here, instead of identifying specific airborne organic species complexed with metals, we employed C18 separation to quantify the total organic-complexed fraction of water-soluble Fe and Cu in ambient PM, and we fractionated the metals into different groups based on their relative hydrophobicity. To further investigate the effect of organic

complexes on metals' oxidative stress, we chose SRFA as a proxy of ambient HULIS, and assessed the potential impact of Fe(II)-SRFA and Cu(II)-SRFA complexes from the endpoints of $\cdot\text{OH}$ generation, consumption of antioxidants and Fenton reaction. The study presents a novel scheme to characterize the complexation state of PM-borne Fe and Cu. The interaction of SRFA with Fe(II) and Cu(II) in all the acellular toxicity assays provides insights into the possible effect of ambient metal-organic complexes on the PM-borne oxidative stress.

CHAPTER 2: MATERIAL AND METHODS

2.1 Reagents

Iron(II) sulfate heptahydrate ($\geq 99.0\%$), 3-(2-Pyridyl)-5,6-diphenyl-1,2,4-triazine-p,p'-disulfonic acid monosodium salt hydrate (ferrozine, 97%), copper(II) sulfate pentahydrate ($\geq 98.0\%$), bathocuproine (96%), hydroxylamine hydrochloride (HA, 99.999%, trace metal grade), nitric acid (67-70%, trace metal grade), sodium hydroxide (99.99% trace metal basis), citric acid ($\geq 99.5\%$), L-ascorbic acid ($\geq 99\%$), citric acid ($\geq 99.5\%$), L-glutathione reduced ($\geq 98.0\%$), uric acid ($\geq 99\%$), DL-dithiothreitol ($\geq 98\%$, TLC), phthaldialdehyde ($\geq 97\%$) were obtained from Sigma-Aldrich Co. (St. Louis, MO). Phosphate-buffered saline (PBS) was bought from Mediatech Inc. (Manassas, VA). Methanol (ACS) was obtained from Fisher Scientific Inc. (Pittsburgh, PA). Disodium terephthalate (TPT, 99+%) was purchased from Alfa Aesar Co. (Haverhill, MA). Dimethyl sulfoxide (DMSO, ACS) and Hydrogen peroxide (30% solution, ACS) were bought from Macron Fine Chemicals Co. (Center Valley, PA). Suwanne river fulvic acid (SRFA standard II, 2S101F) was purchased from International Humic Substances Society (IHSS). C18 silica gel (premium grade) was obtained from Sorbent Technologies Inc. (Norcross, GA).

2.2 Preparation of stock solutions

The stock solutions of metals were made in Milli-Q water (0.11mg/mL and 0.13mg/mL for Fe and Cu, respectively) weekly and stored at 4°C. SRFA stock was prepared in Milli-Q water (1mg/mL) every time prior to experiment. The stock solution of ferrozine was made in Milli-Q water (2.55 mg/mL) monthly and stored at 4 °C in an amber bottle. HA (800 mg/mL) solution was prepared in an acid-cleaned amber bottle. Iron(II) stock solution (1 g/L) was prepared every week and acidified to maintain a pH=1. The stock solution of bathocuproine was prepared in methanol

(0.36 mg/mL) and stored in an amber bottle at 4°C. The surrogate lung fluid (SLF) consists of four different antioxidants. Its preparation follows Charrier et al.³⁷ protocol. Briefly, the stock solutions of L-ascorbic acid (Asc, 12 mM), citric acid (Cit, 12 mM) and L-glutathione (GSH, 12 mM) were prepared in phosphate-buffered saline (PBS) every week. The stock solution of uric acid (UA, 12 mM) was dissolved in 1M NaOH and prepared fresh before every experiment. Final concentrations in the SLF were 200 µM Asc, 300 µM Cit, 100 µM GSH and 100 µM UA. TPT (60mM) was made in PBS. DMSO (100 mM) was made in Milli-Q water. The stock solution of DTT was prepared in Milli-Q water (10mM), while the concentration in the reaction vial is 100 µM. The stock solution of OPA was prepared in methanol (0.2M) every time prior to the experiment.

2.3 Ambient PM sampling

Thirty ambient PM_{2.5} samples were collected using a high volume sampler (HiVol, Thermo Anderson, nominal flow rate 1.13 m³ min⁻¹) in four different seasons of the year, i.e. spring (March-April 2017, N=10), summer (July-August 2017, N=8), fall (October-November 2017, N=7), winter (December 2017-February 2018, N=5). The sampler was located on the roof of a parking garage on UIUC campus, which is adjacent to a major four-lane street (University Avenue) in Urbana, IL. Prebaked (at 550 °C) quartz filters (8 in. × 10 in., Pallflex Tissuquartz, Pall Life Sciences) were used for sampling. The sampling duration for these samples varied between 48 – 72 hours depending on the seasons. Exact dates of sampling with the duration of each sample are provided in Table 1 in Appendix A. Three field blanks were also collected and stored with the samples in a freezer (-20°C) until analysis.

2.4 PM extraction

Circular sections of 0.625'' diameter were punched from the PM laden Hi-Vol filters (including blanks). These punches were extracted by sonication for 30 minutes separately in Milli-Q water (resistivity = 18.2 MΩ/cm) and 50% methanol (in Milli-Q water) solution. Two punches per 10 mL solvent were extracted for Fe measurement and 1 punch per 10 mL for Cu measurement, and all the extracts were filtered by PTFE 0.45 μm pore syringe filters (Fisher brand). 50% methanol solution was used because pure methanol interferes in the absorbance measurement for both Fe and Cu analysis. Tests conducted using different concentrations of the methanol in DI (5%, 15%, 20%, 30%, 35%, 40%, and 50% in Milli-Q water) to extract the PM filters showed that the concentration of Fe reached saturation at 50% methanol (Figure 9 in Appendix A). Therefore, 50% methanol solution was chosen to extract any additional water-soluble Fe in ambient PM, which could have been dissolved in methanol. All the experiments in this section were conducted in duplicates.

2.5 C18 fractionation of PM samples and Fe and Cu standards and their mixtures with SRFA

The fractionation of PM samples, Fe and Cu standards and their mixtures with SRFA basically follows the procedures shown in figure 1. Additional punches (0.625'' diameter) were separately extracted in Milli-Q water for Fe and Cu fractionation over C18 column (four punches for Fe and two punches for Cu fractionation, per 20 mL water). After filtration by syringe filters, the extracts were divided into two identical samples (10 mL each). One was directly analyzed for Fe and Cu concentrations, while the other was passed through a C18 column for fractionation. The C18 columns were preconditioned by first rinsing the resin with 10 mL methanol, followed by 10 mL of 0.5% HNO₃, and finally 10 mL Milli-Q water. Methanol was used to activate the column,

and HNO₃ was used to remove any metal contamination. Iron (0.4 μM) and copper (0.8 μM) standards, and their mixtures with SRFA, i.e. Fe (0.4 μM) +SRFA (4 μg/mL) or Cu (0.8 μM) + SRFA (8 μg/mL) were also passed through the column in parallel with the PM extract. After the extract effluent (passed-through fraction of the original extract) was collected, 50% methanol solution was passed through the column, followed by 0.5% HNO₃. The eluate of HNO₃ was neutralized by NaOH to adjust the pH ~7. A similar fractionation protocol was employed for pure Fe and Cu standards and their mixtures with SRFA passed through the columns. Both the effluent and eluates (i.e. 50% methanol and 0.5% HNO₃) were analyzed for Fe and Cu. Blank groups were conducted for each fraction by passing both Milli-Q water and extracts of field blank filters through a C-18 column, collecting the effluent and eluting the column with 50% methanol followed by 0.5% HNO₃.

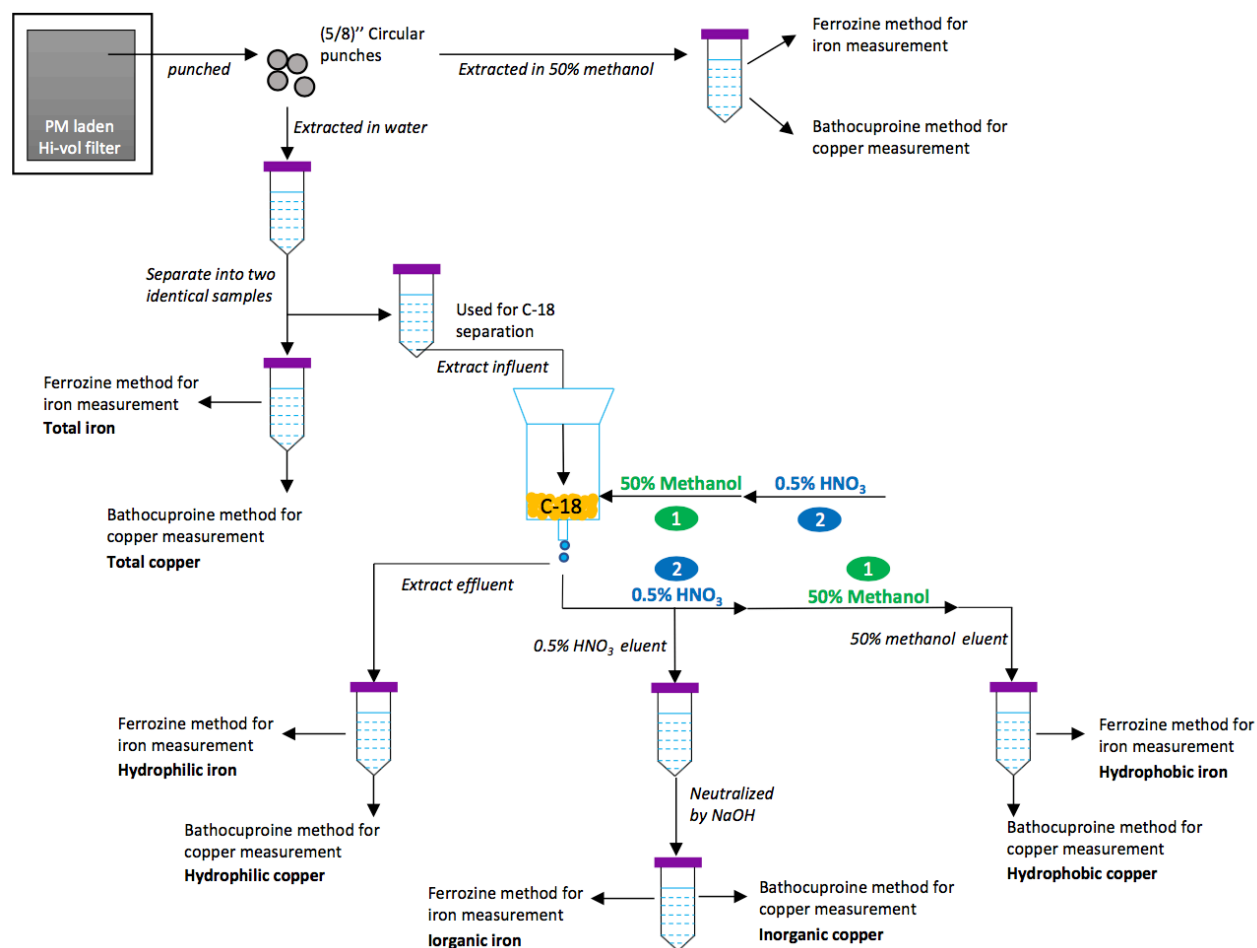


Figure 1. Procedures of C18 fractionation of ambient PM samples

2.6 Iron and copper analysis

Iron in the samples was analyzed following the protocols of ferrozine method.^{52,53} All the glassware used in iron and copper measurements were soaked in 2.5N hydrochloric acid overnight and then rinsed with Milli-Q water three times. 100 μL of ferrozine stock was added to 10 mL of the sample (i.e. PM extracts Fe+SRFA mixture, their hydrophilic effluents, and methanol or HNO_3 eluates) followed by 20 μL HA. The magenta-colored ligand formed by Fe(II) and ferrozine absorbs light at 562 nm, and was measured by an online miniature spectrophotometer (Ocean Optics, Dunedin FL), which consists of an ultraviolet-visible-near-infrared (UV-Vis-NIR) light

source, a multi wavelength light detector, and a liquid waveguide capillary cell (World Precision Instruments, Sarasota, FL). Calibration with known concentrations (1 $\mu\text{g/L}$, 2.5 $\mu\text{g/L}$, 5 $\mu\text{g/L}$, 10 $\mu\text{g/L}$, and 20 $\mu\text{g/L}$) of freshly prepared Fe(II) standard was conducted once in a week and the calibration equation was used to calculate the iron concentration in the samples. The calibration curve is shown in Figure 10 in Appendix A.

Cu in the samples was measured following bathocuproine method by adding HA (50 μL) and bathocuproine (100 μL).⁵⁴ After Cu(II) was reduced by HA, Cu(I) would form an orange-colored complex with bathocuproine, which has a characteristic absorbance at a wavelength 484nm, and thus easily measured by the same spectroscopy setup used for Fe measurement. The calibration was conducted every week with freshly made bathocuproine solution and Cu standards of different concentrations (6.4 $\mu\text{g/L}$, 12.7 $\mu\text{g/L}$, 19.1 $\mu\text{g/L}$, 25.4 $\mu\text{g/L}$, and 38.1 $\mu\text{g/L}$). The calibration curve is shown in Figure 11 in Appendix A. The blank groups for each type of the sample were similarly analyzed for the concentration of Fe and Cu and all the data was blank corrected by subtracting corresponding blank concentration (i.e. Milli-Q water for Fe and Cu standard, field blank for PM sample, effluent and eluate of blanks for effluent and eluate of the samples, respectively). The concentration of Fe and Cu in any of these blanks were less than 0.30 $\mu\text{g/L}$ for Fe and 1.81 $\mu\text{g/L}$ for Cu, which were substantially lower levels than PM samples (concentration ranges 0.60 – 48.3 $\mu\text{g/L}$ and 2.95 – 83.9 $\mu\text{g/L}$ for Fe and Cu, respectively).

2.7 OP measurement

The effect of complexation of metals (Fe or Cu) with organic compounds on oxidative potential (OP) was quantified by measuring flowing endpoints: $\cdot\text{OH}$ generation in a surrogate lung fluid (SLF) and DTT, ascorbate and glutathione consumption SLF, and $\cdot\text{OH}$ generation from H_2O_2 .

Each of these endpoints is described below.

2.7.1 ·OH generation in SLF, DTT and H₂O₂

The ·OH measurement followed Xiong et al.¹⁶ protocol. TPT was used as an ·OH probe in this fluorescence-based approach. Due to the high stability (<3% decay in 36 h⁵⁵) of the fluorescent product 2-hydroxyterephthalic acid (2-OHTA), formed by the reaction between TPT and ·OH, its formation was used to represent the generation of hydroxyl radical. The reaction vial contained 12 mL reaction mixture, consisting of 7 mL samples, 2 mL PBS, 2 mL TPT and 1 mL antioxidant (i.e. SLF or DTT) or 1 mL H₂O₂ solution (10 μM, 20 μM and 50 μM in the reaction vial). All the sample setup discussed in sections 2.6 and 2.7 were conducted as follows: 1 μM Fe, 1 μM Cu, 10 μg/mL SRFA, Fe-SRFA mixture and Cu-SRFA mixture. The reaction vial was kept in a water bath (StableTemp by Cole-Parmer, Vernon Hills, IL) at 37 °C. After fixed time intervals (0 min, 20 min, 40 min, 60 min, 80 min), 2 mL of samples was withdrawn and mixed with 1 mL to quench formation of 2-OHTA. The fluorescence intensity of 2-OHTA was measured by a Horiba Fluoromax-4L spectrofluorometer (Horiba Scientific; Edison, NJ) at excitation/emission wavelengths of 310/425 nm, respectively. The concentration of 2-OHTA in the samples was calculated by conducting a calibration with known concentrations of 2-OHTA prior to the experiment. All the experiments in this section were conducted in triplicates.

2.7.2 Ascorbic acid (AA) consumption and glutathione (GSH) consumption in SLF

Ascorbic acid has a characteristic absorbance at a wavelength 265 nm in a neutral aqueous solution.⁵⁶ Here we use a simple spectroscopic method to quantify the consumption rate of AA in SLF by determining the remaining AA at different time points. In order to exclude the possible

interference of other antioxidants in AA measurement, we recorded the absorbance of SLF at 265nm with different concentrations of antioxidants: AA fixed at 200 μM ; Cit at 300 μM , 250 μM , 200 μM and 150 μM ; UA and GSH at 100 μM , 70 μM , 50 μM and 30 μM . The result is shown in Table 2 in Appendix A, and it denotes that the variation of Cit, UA and GSH exerts negligible influence on the measurement of AA. The initial concentration of AA in the reaction vial was 200 μM , while the initial concentrations of other antioxidants were 300 μM (Cit), 100 μM (GSH) and 100 μM (UA). A reaction vial consists of 9 mL sample, 950 μL PBS and 100 μL SLF. An aliquot of 50 μL from the reaction vial was withdrawn and diluted to 10 mL at time points of 0 min, 20 min, 40 min, 60 min, 80 min, and then the absorbance was determined following the same protocol discussed in section 2.6. The reaction vials were incubated in a Thermomixer (Eppendorf, Hamburg, Germany) at 37 $^{\circ}\text{C}$ and 500 rpm. A blank sample was included in each of the experiments. The calibration was conducted with AA concentrations of 0.1 μM , 0.2 μM , 0.4 μM , 0.8 μM , 1.0 μM , in the presence of Cit, GSH and UA, and is shown in Figure 12 in appendix A.

We used a fluorescent method to quantify the consumption rate of GSH. In the assay, o-phthalaldehyde (OPA) reacts exclusively with GSH to generate strong fluorescent product, while OPA itself has a very low fluorescence background.⁵⁷ The GSH measurement follows the GSH, GSSG and Total Glutathione Assay Kit protocol.⁵⁸ Here we recorded the GSH consumption rate in SLF, with the presence of other three antioxidants. The reaction vial contained 3 mL sample, 1 mL PBS and 1mL SLF, with GSH concentration being 100 μM . The reaction vials were incubated in a water bath a 37 $^{\circ}\text{C}$. At time points of 0 min, 10 min, 20 min, 30 min and 40 min, 50 μL aliquot of the reaction vial was added to 4.9 mL PBS, along with 50 μL OPA to form a fluorescent product, the intensity of which was measured by a Horiba Fluoromax-4L spectrofluorometer (Horiba Scientific; Edison, NJ) at excitation/emission wavelengths of 360/435 nm, respectively. The

calibration of GSH concentration was conducted in presence of Cit, AA and UA, with GSH concentrations as 0.05 μM , 0.25 μM , 0.50 μM , 0.75 μM and 1.0 μM , and is shown in Figure 13 (appendix A). All the experiments were conducted in duplicates.

2.8 Statistical analyses

Interaction factors (IFs) were calculated to evaluate the synergistic/antagonistic interactions in the mixtures of metals (Fe and Cu) and SRFA⁴⁴. IF is defined as the ratio of the activity (either $\cdot\text{OH}$ generation or AA/GSH consumption) of the mixture (A + B) over the sum of their individual activities:

$$\text{IF}_{A,B} = \frac{R_{A,B}}{R_A + R_B}$$

Where R_A , R_B and $R_{A,B}$ represents activity of the substances A and B and the mixture of A and B, respectively.

The standard deviation (SD) in IF is calculated as

$$\text{SD}(\text{IF}_{A,B}) = \text{IF}_{A,B} \sqrt{\frac{[\text{SD}(R_{A,B})]^2}{R_{A,B}^2} + \frac{[\text{SD}(R_A)]^2 + [\text{SD}(R_B)]^2}{(R_A + R_B)^2}}$$

CHAPTER 3: RESULTS AND DISCUSSION

3.1 Concentration of Fe and Cu in water versus methanol extracts

Figure 2 shows the concentration of Fe and Cu in PM samples as extracted by water and 50% methanol. For most of the samples in spring, fall and winter (with exceptions of S7, S9 and S23 in Fe), both Fe and Cu in ambient PM were more effectively dissolved in 50% methanol than in Milli-Q water. The increase in solubility of Fe and Cu in methanol over water was $35\pm 27\%$ and $52\pm 39\%$ (on average), respectively. Fe concentration in the summer samples showed a reverse trend, where water extract averaged $70\pm 41\%$ higher than 50% methanol extract. However, Cu was higher ($33\pm 20\%$ on average) in 50% methanol than water for summer samples.

Given the lower polarity of methanol than water, the free or inorganic metals are expected to be less soluble in 50% methanol than Milli-Q water. For example, Urréjola et al.⁵⁹ quantified an exponential decrease in solubility of copper (II) sulfate with increasing mass fraction of ethanol in ethanol-water mixtures, with copper concentration around 10^{-1} M. However, considering relatively low concentrations of Fe and Cu in our PM water-soluble extracts (<1 μM), it is reasonable to assume a similar solubility of any free or inorganic metals (i.e. Fe and Cu) in both methanol and water. Therefore, any difference in Fe or Cu extracted in methanol versus water, is attributed to the fraction of these metals complexed with organic compounds, which could have a wider range of solubility profiles based on their hydrophobicity or polarity. For example, Cu has been reported to possess strong affinity for natural occurring organic matter in the atmosphere (e.g. aerosols and rainwater).^{26,60,61} Okochi et al.³⁵ found that ambient Cu in the soluble fraction was complexed with macromolecules (e.g. fulvic and humic acids), which exhibited strong hydrophobicity. On the other hand, Fe is shown to be associated with both humic-like substances, which are strongly hydrophobic, and hydrophilic compounds, e.g. oxalic acid, malonic acid.⁶²

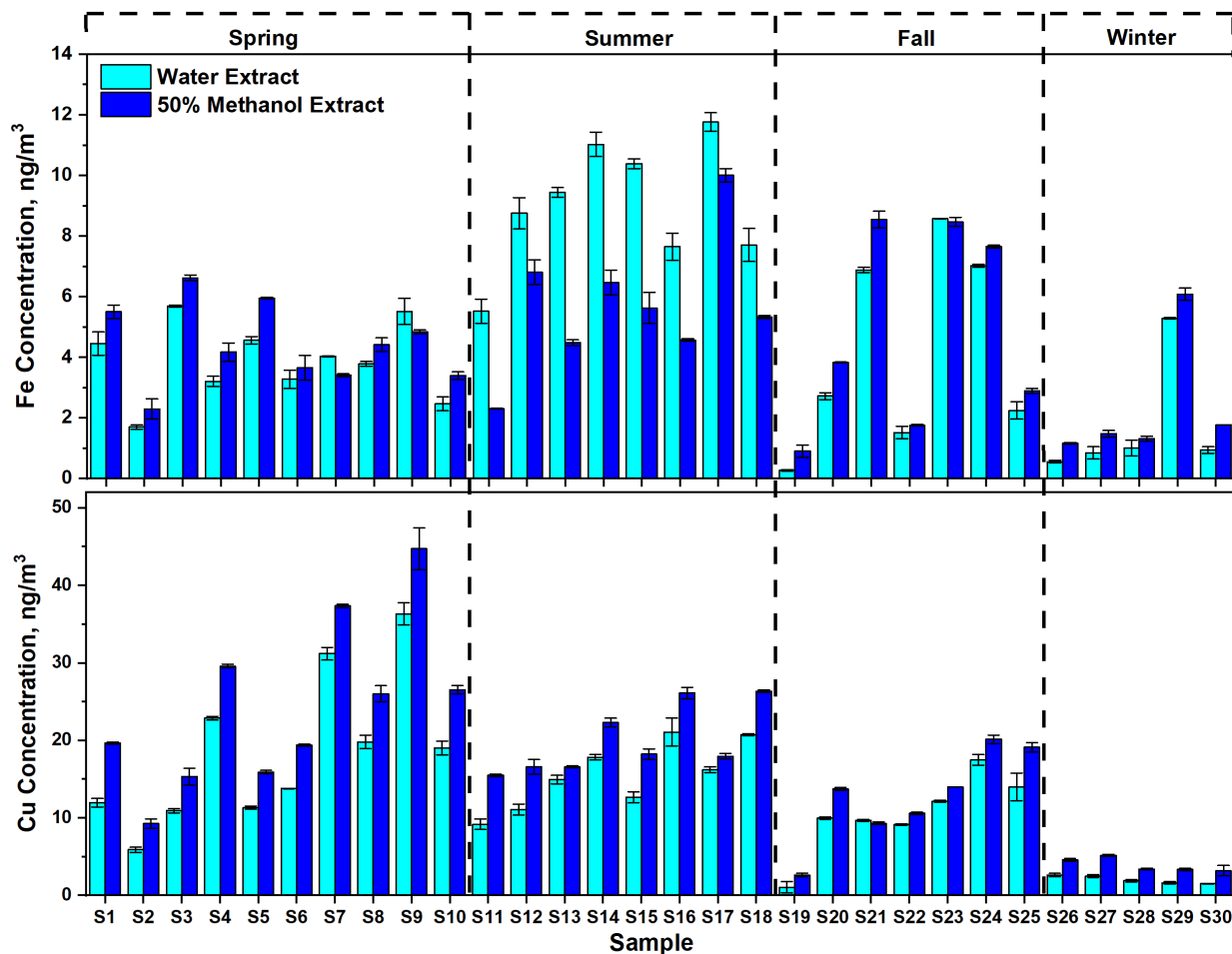


Figure 2. Comparison of Fe and Cu concentrations in water and 50% methanol extracts of ambient PM samples in four seasons

To further understand the relative complexation of Fe and Cu with hydrophobic and hydrophilic compounds, a novel fractionation scheme was used for PM water extract (discussed next) based on the separation capability of C18 resin.

3.2 C18 fractionation of PM samples and SRFA

Here, we employed a C18 separation method to quantify ambient Fe and Cu associated with three fractions, i.e. complexed with hydrophilic organic compounds, complexed with hydrophobic organic compounds and free or inorganic form. To validate our fractionation scheme, Fe and Cu

standards ($0.4 \mu\text{M Fe}^{2+}$ and $0.8 \mu\text{M Cu}^{2+}$) were passed through a preconditioned C18 column as control groups. Figure 3 shows the fractionation result of Fe and Cu standards. Only $11 \pm 1\%$ Fe and $6 \pm 1\%$ Cu came off in the effluent of the standards. Out of $>90\%$ fraction retained on the column, only $6 \pm 3\%$ Fe and $12 \pm 2\%$ Cu were eluted in 50% methanol. Mackey^{63,64} has shown that inorganic (i.e. free metal ions and metals complexed with inorganic compounds) Fe and Cu would be strongly adsorbed by the uncapped, free silanol groups on C18 resin, which is verified by these experiments. Finally, rinsing the column with HNO_3 eluted $>80\%$ of both of these metals in HNO_3 eluates.

Based on these results, it could be inferred that for ambient PM extract, any Fe or Cu coming off in the effluent of PM extracts was complexed with the hydrophilic organic compounds, while free or inorganic metals and the fraction complexed with hydrophobic organic compounds were retained on the column. The fraction complexed with hydrophobic organic compounds can be eluted from the column by passing 50% methanol solution, which has been shown to successfully elute copper-organic complexes from seawater samples after passing them through a C18 column.⁶⁵ Thus, any metal retained on the C18 column after methanol elution should be free or complexed with inorganic substances. For example, some previous modeling result using MINTEQ²³ indicated that in ambient PM, nitrate could be an effective inorganic agent to chelate Fe^{2+} , and that Cu^{2+} could be chelated with the chloride. These free or inorganic metals can be eluted by passing 0.5% HNO_3 as shown by Sunda et al.⁶⁶

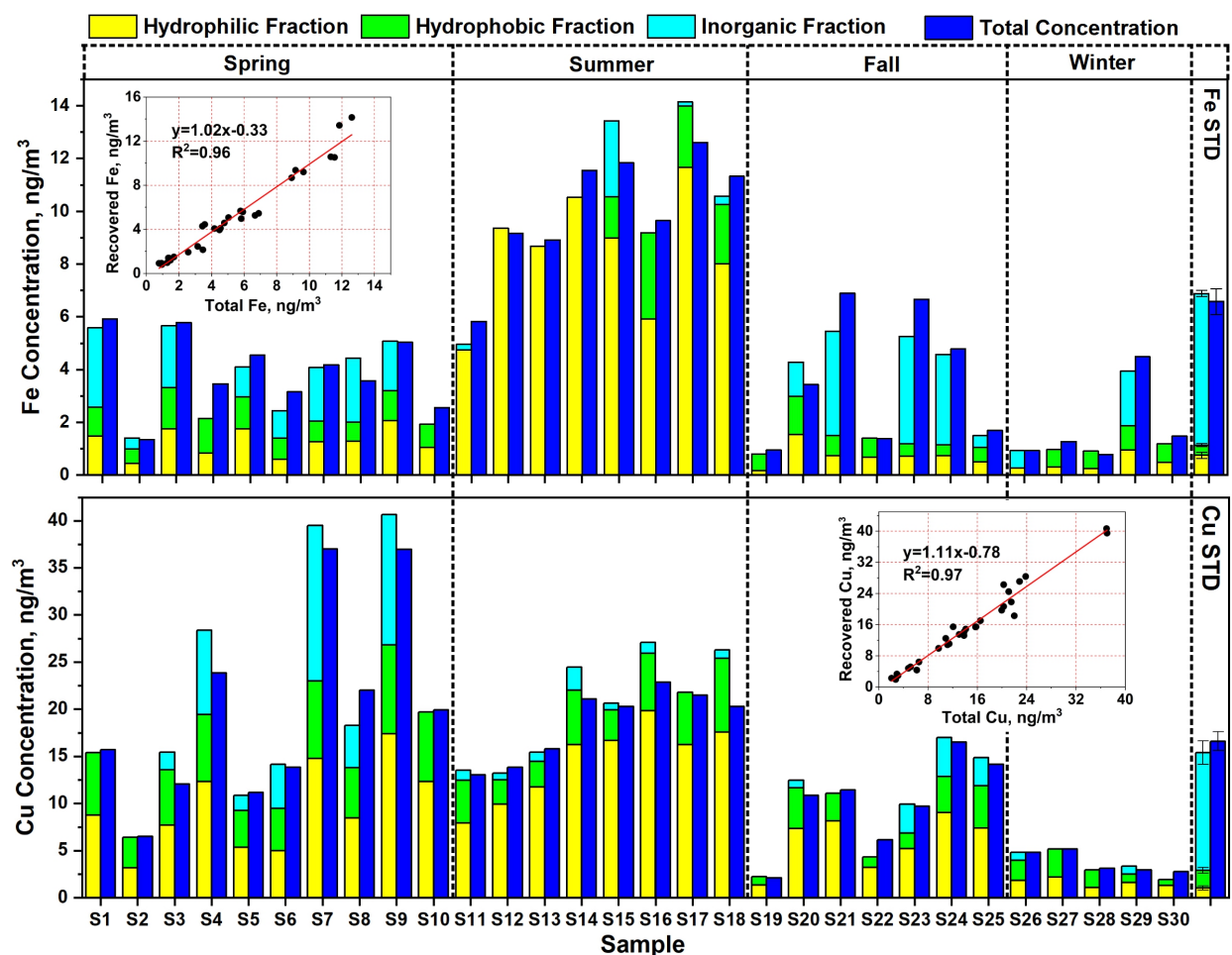


Figure 3. C18 fractionation of Fe and Cu standards solutions, and Fe and Cu in ambient PM samples in four seasons

The results obtained from the C18 fractionation of ambient samples are also shown in Figure 3. It is evident that most of the Fe and Cu ($74 \pm 27\%$ for Fe and $88 \pm 13\%$ for Cu; average of all samples) in ambient samples were complexed with the organic compounds, while only a minor fraction ($<30\%$) was free (or complexed with inorganic compounds). Overall, percentage of the metals with the hydrophilic organic compounds ($46 \pm 27\%$ for Fe and $57 \pm 14\%$ for Cu) outweighs the fraction complexed with the hydrophobic organic compounds ($28 \pm 22\%$ for Fe and $31 \pm 11\%$ for Cu) in the water-soluble extracts of our samples. Mass balance for these metals, i.e. correlation between metal measured in the effluent of the PM samples (complexed with hydrophilic organic

compounds) + measured in 50% methanol eluates (complexed with hydrophobic organic compounds) + 0.5% HNO₃ eluates (free or complexed with inorganic compounds) and total water-soluble metals measured in the original extract is also shown as an inset in Figure 3. The excellent correlation ($R^2=0.96$ and slope=1.02 for Fe; $R^2=0.97$ and slope=1.11 for Cu) essentially demonstrates the robustness of our fractionation scheme to recover all the fractions.

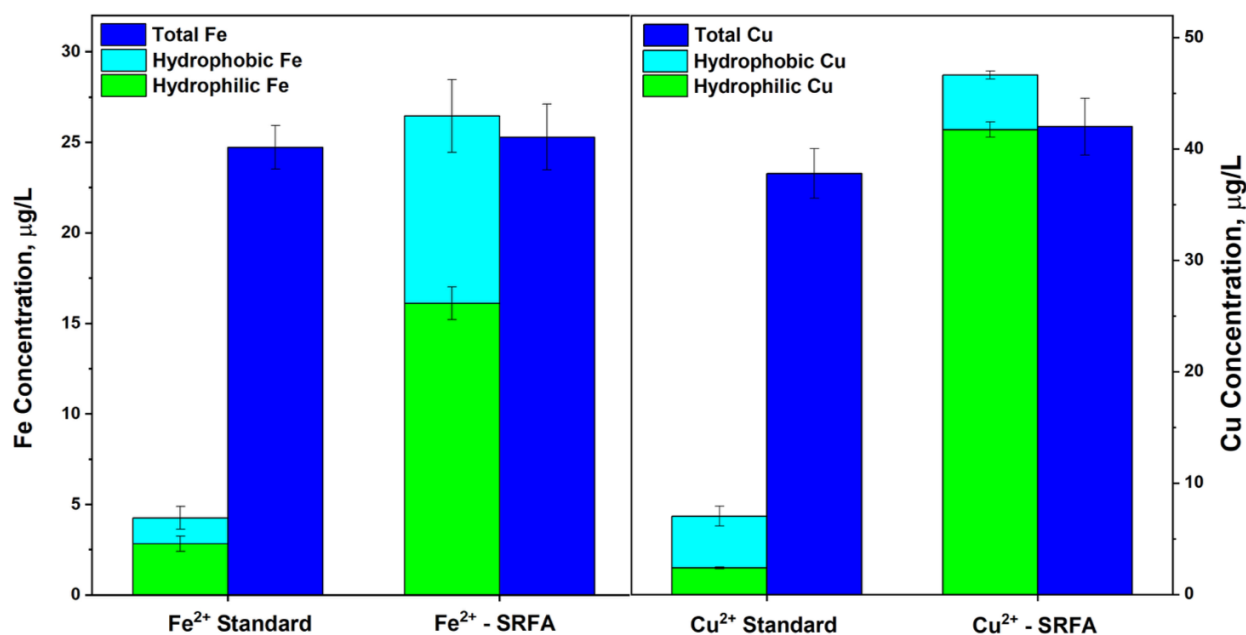


Figure 4. C18 fractionation of Fe and Cu standard solutions, and the mixture of Fe/Cu standard solutions with SRFA

To further validate our fractionation scheme to quantify the fractions of metals associated with hydrophobic and hydrophilic compounds, we passed a mixture of SRFA and metals (i.e. 0.4 µM Fe(II) + 4 µg/mL SRFA and 0.8 µM Cu(II) + 8 µg/mL SRFA) through the C-18 column and recovered the various fractions by collecting the effluent, methanol eluates and HNO₃ eluates. The modeling results from Gonzalez et al.⁴³ have shown its excellent complexation efficiency with both Fe and Cu. Consistent with that study, our fractionation results of Fe-SRFA mixture (Figure

4) show that almost all of the Fe and Cu are complexed with SRFA. Hydrophilic fraction of SRFA dominated the complexation of both Fe ($61\pm 3\%$) and Cu ($89\pm 1\%$) in these experiments as well, which is consistent with ambient samples.

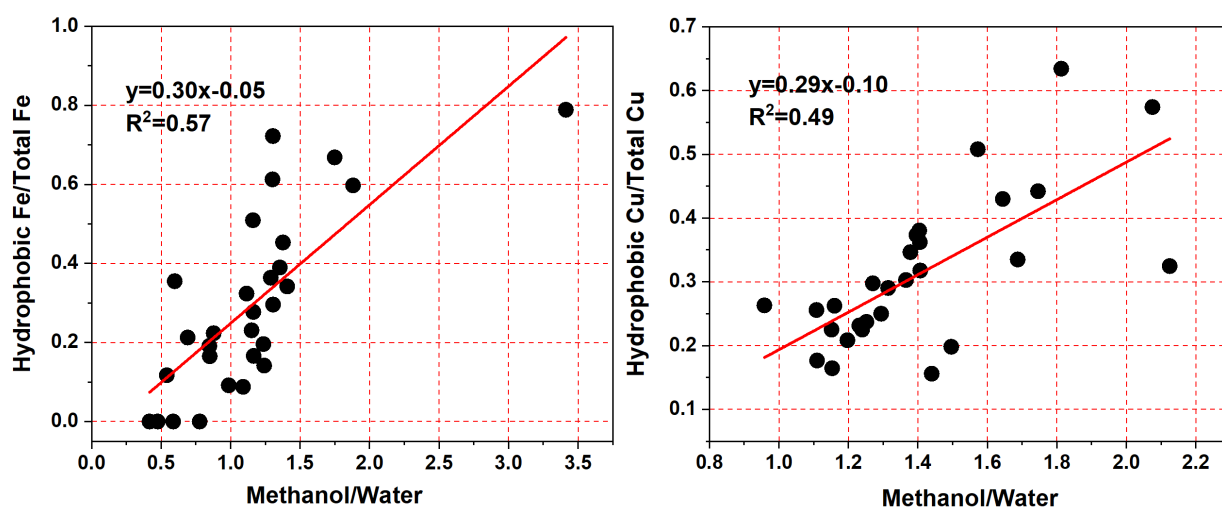


Figure 5. Correlation between the ratio of hydrophobic Fe/Cu to total Fe/Cu, and the ratio of 50% methanol-soluble Fe/Cu to water-soluble Fe/Cu

The C18 fractionation can partially help to understand the water versus 50% methanol extraction results of these ambient samples (Figure 2). The samples with more Fe or Cu dissolved in water than 50% methanol (e.g. the summer samples) appear to have an overall higher fraction complexed with the hydrophilic organic compounds. To further explore this, we plotted additional percentage of metals dissolved in 50% methanol over water, versus percentage fraction complexed with hydrophobic organic compounds (as obtained from C-18 column). As shown in Figure 5, there is a decent correlation ($R^2>0.50$) between these fractions. The characterization of atmospheric water-soluble organic compounds conducted in past studies in Atlanta have shown a more aliphatic fraction in summer (59%) than winter (45%).⁴⁹ The strongly hydrophilic

compounds such as dicarboxylic acids (e.g. oxalic acid, malonic acid and succinic acid) are known to efficiently complex Fe,^{23,62} probably making Fe more soluble in water than methanol.

3.3 ROS measurement

3.3.1 ·OH generation from Fe, Cu and SRFA

To investigate the toxicological relevance of the complexation of metals, particularly Fe and Cu with the organic compounds, we measured the capability of the complexes of Fe and Cu with SRFA to generate hydroxyl radical. Fe, Cu and SRFA were also tested individually to compare the sum of their ·OH generating activities with that of their complexes (i.e. Fe-SRFA and Cu-SRFA complexes). Two different assays (i.e. surrogate lung fluid assay and DTT assay) were chosen for the ·OH generation experiments. Fe-SRFA and Cu-SRFA complexes were formed by mixing 10µg/mL SRFA with 1µM Fe(II) and 1µM Cu(II), respectively, and keeping the mixtures at room temperature for 10 minutes. Figure 6 shows the ·OH generation capability of the individual compounds and the complexes in two assays. The ·OH generation rate in both assays was much higher for Fe-SRFA complex than the sum of Fe and SRFA (mixture/sum = 4.35 ± 0.35 and 5.86 ± 0.30 for SLF and DTT assays, respectively), clearly showing a strong synergistic effect for Fe-SRFA complex in ·OH generation. However, SRFA-Cu complex shows similar ·OH generation activity as obtained from the sum of their individual activities (SLF: mixture/sum = 1.27 ± 0.17 ; DTT: mixture/sum = 0.98 ± 0.37). The SLF assay has been a conventional method for measuring the ROS generation potential of ambient aerosols^{15,37}. Several components of the ambient PM, which include both organic compounds (e.g. quinones) and metals (e.g. Fe, Cu, Mn) have been shown to generate ·OH radicals in this assay. Xiong et al.¹⁶ developed a new protocol for measuring the ·OH radicals in DTT assay, which is also shown to incorporate the contribution

from both organic compounds and metals. While Cu(II) generally shows higher activity than Fe(II) in SLF and AA assays, it has negligible ability to generate $\cdot\text{OH}$ in DTT, which could be explained by an equimolar complex formed by Cu and DTT, that is incapable to generate any significant ROS.⁶⁷

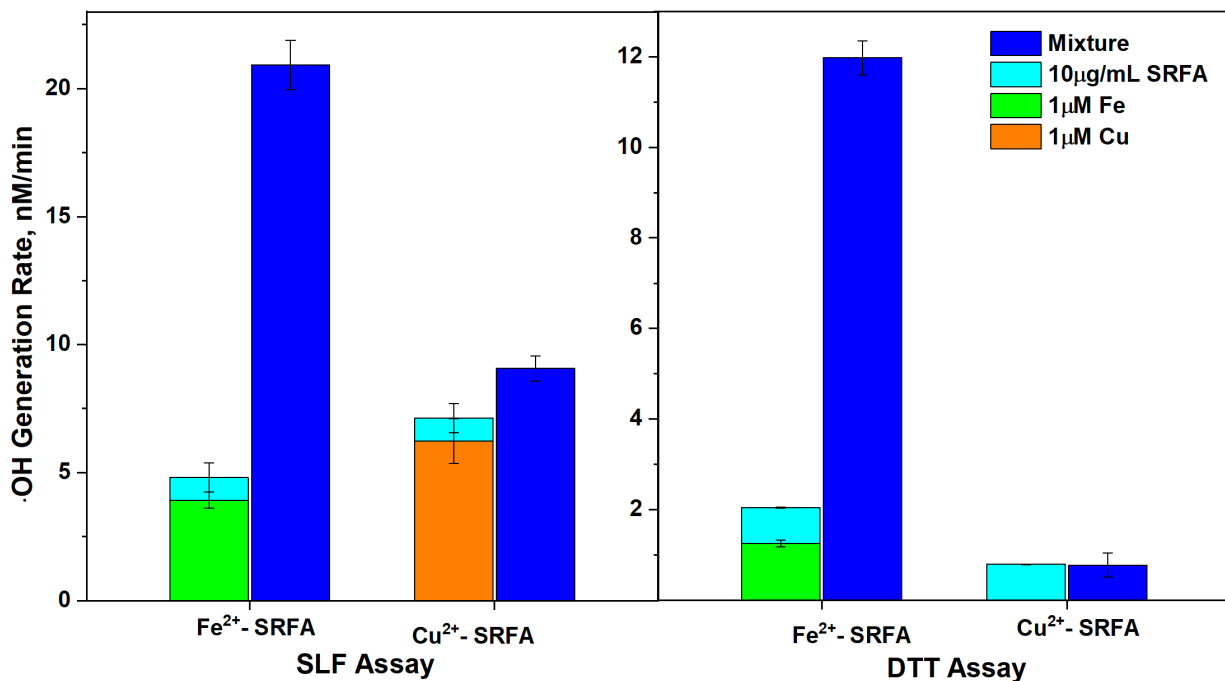


Figure 6. Rate of $\cdot\text{OH}$ generation of the mixture of SRFA with Fe/Cu and their individual compounds in SLF and DTT

Different mechanisms have been proposed to explain the synergistic effects of Fe(II) and SRFA in generating $\cdot\text{OH}$. Based on modeling results, Gonzalez et al.⁴³ proposed that Fe-SRFA complexes could enhance Fe-mediated reduction of O_2 to O_2^- and conversion of H_2O_2 to $\cdot\text{OH}$ in SLF, thus speeding $\cdot\text{OH}$ production as a net result. According to our previous study,⁴⁴ however, this synergistic effect could be attributed to enhanced destruction of H_2O_2 formed in the SRFA-DTT system by Fe. Since SRFA shows notable activity of generating $\cdot\text{OH}$ in both lung antioxidants and DTT (0.89 ± 0.08 nM/min and 0.79 ± 0.01 nM/min in SLF and DTT, respectively), Fe(II) could

promote the total $\cdot\text{OH}$ yield by efficiently converting H_2O_2 generated by SRFA-catalyzed DTT or Asc oxidation. Similar mechanism was also indicated to account for the synergistic effect between Fe(II)/Fe(III) and quinones.¹⁶ It is still unclear whether these two mechanisms are competitive, or one dominates the other. In addition, none of previous studies has reported the Fe-SRFA synergy to be as prominent as our result (interaction factor up to 5.86 ± 0.43 compared to 1.40 ± 0.13 ⁴⁴ and less than 2⁴³). Moreover, the difference pattern of Cu-SRFA from Fe-SRFA interaction in $\cdot\text{OH}$ production might implicate alternative explanation for the additive effect of Cu and SRFA. To explore these issues, we disassembled $\cdot\text{OH}$ generation into consumption of antioxidants and Fenton reaction (i.e. conversion of H_2O_2 to $\cdot\text{OH}$) and studied the effect of Cu-SRFA and Fe-SRFA complexes in these two processes.

3.3.2 Consumption of antioxidants from Fe, Cu and SRFA

Figure 7 shows the AA consumption rate in SLF and GSH consumption rate in SLF, of individual compounds and their complexes. Apparently, the simple spectroscopic and fluorescent methods we used could not quantify the relatively low activity of Fe consuming AA or GSH. The results of $1 \mu\text{M}$ Fe in both assays were below limit of detection ($\text{LOD}_{\text{AA-SLF}} = 0.20 \text{ nmol/min}$, $\text{LOD}_{\text{GSH-SLF}} = 0.15 \text{ nmol/min}$). The relative capacity of Fe and Cu to consume AA, is consistent with the finding of Distefano et al.,¹⁴ where Cu is 20 times more active than Fe in AA consumption. Meanwhile, $10 \mu\text{g/mL}$ SRFA shows negligible ability to consume AA in SLF ($0.39 \pm 0.01 \text{ nmol/min}$), and limited activity to consume GSH in SLF ($1.73 \pm 0.40 \text{ nmol/min}$). Under no circumstance, Fe and SRFA demonstrate any noticeable synergistic effect as observed in $\cdot\text{OH}$ generation. Due to the limitation of our techniques, it is difficult to conclude whether the Fe-mediated reduction of O_2 to O_2^- through destruction of AA or GSH was enhanced by Fe-SRFA

complexes, as indicated by Gonzalez et al.⁴³ In light of the limited activity of Fe-SRFA mixture in AA or GSH consumption, however, the interaction of Fe-SRFA during this process is highly unlikely to be responsible for the significant enhancement of overall $\cdot\text{OH}$ yield, thus suggesting that Fenton reaction be the driving process. On the other hand, Cu-SRFA interaction in consumption of antioxidants shows completely different trend from Fe-SRFA. Consistent with previous observations, antagonistic effect of Cu-SRFA was observed in AA consumption in SLF (mixture/sum = 0.66 ± 0.05) and GSH consumption in SLF (mixture/sum = 0.38 ± 0.04), suggesting a significant inhibition of O_2^- or H_2O_2 formation. Our finding is supported by DTT consumption catalyzed by Fe, Cu and SRFA,⁴⁴ where Fe-SRFA shows additive effect (mixture/sum = 0.81 ± 0.25) and Cu-SRFA shows antagonistic effect (mixture/sum = 0.64 ± 0.18), except that SRFA consumes DTT more efficiently. Therefore, although the inactivity of SRFA in AA consumption implies that Fe-SRFA interaction in Fenton reaction be responsible for the synergy of $\cdot\text{OH}$ generation, the noticeable amount of H_2O_2 generated by SRFA oxidizing DTT still make way for the explanation of sequential nature. In this sense, the Fe-SRFA and Cu-SRFA interactions need to be further addressed in Fenton reaction.

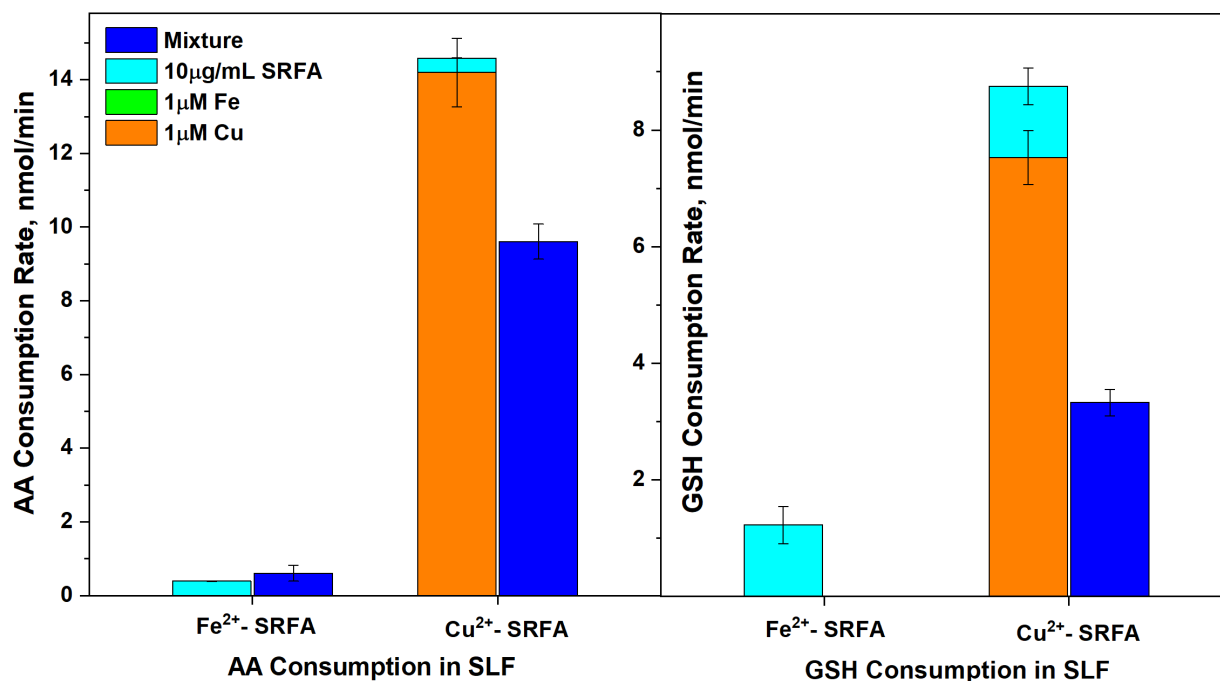


Figure 7. Rate of AA and GSH consumption in SLF by the mixture of SRFA with Fe/Cu and their individual compounds

3.3.3 Fenton reaction catalyzed by Fe, Cu and SRFA

Figure 8 shows the $\cdot\text{OH}$ generation rate converted from 10 μM , 20 μM and 50 μM H_2O_2 by individual compounds and their mixture. Xiong et al.¹⁶ measured the H_2O_2 concentration generated by 0.25 μM quinones in DTT assay, ranging from 0 to 20 μM during a 30-minute period. Surprisingly, Fe^{2+} shows negligible ability to convert H_2O_2 to $\cdot\text{OH}$ under all H_2O_2 concentrations ($\cdot\text{OH}$ generation rate 0.04 ± 0.03 nM/min, 0.11 ± 0.15 nM/min, 0.19 ± 0.08 nM/min for 10 μM , 20 μM and 50 μM H_2O_2 , respectively) compared to Cu^{2+} ($\cdot\text{OH}$ generation rate 0.92 ± 0.04 nM/min, 1.67 ± 0.28 nM/min, 4.54 ± 0.09 nM/min for 10 μM , 20 μM and 50 μM H_2O_2). In contrast, Fe^{2+} and SRFA are strongly synergistic in H_2O_2 conversion (mixture/sum = 8.67 ± 0.59 , 6.62 ± 2.31 , 6.32 ± 2.81 for 10 μM , 20 μM and 50 μM H_2O_2 , respectively), whereas Cu^{2+} and SRFA show additive effect in Fenton-like reaction (mixture/sum = 1.05 ± 0.05 , 1.15 ± 0.25 , 1.09 ± 0.01 for 10

μM , 20 μM and 50 μM H_2O_2 , respectively). Therefore, the strong synergistic effect of Fe and SRFA in $\cdot\text{OH}$ generation in the presence of antioxidants, could be attributed to the interaction of Fe and SRFA in Fenton reaction, probably due to the formation of Fe-SRFA complexes. Miller et al.⁶⁸ reported that in the absence of ligands at circumneutral pH, $\cdot\text{OH}$ yield from the peroxidation of inorganic Fe(II) was always below detection limit, consistent with our result showing the inactivity of Fe(II) at pH=7.4 to catalyze $\cdot\text{OH}$ production from H_2O_2 . Contrary to the well-established generation of $\cdot\text{OH}$ in Fenton reaction at lower pH, the Fe(II)- H_2O_2 reaction would produce high valent species of Fe (e.g. Fe(IV)) instead of $\cdot\text{OH}$ at neutral pH.⁶⁹ The result of kinetic modeling³⁸ validates that the H_2O_2 -mediated oxidation of Fe-SRFA complexes serves as the sole source of $\cdot\text{OH}$ in the Fe-SRFA- H_2O_2 system. Accordingly, the organic complexation of Fe(II) could be a prerequisite of $\cdot\text{OH}$ production under circumneutral conditions,⁶⁸ highlighting the significance of metal complexation in altering the oxidative potential of ambient PM.

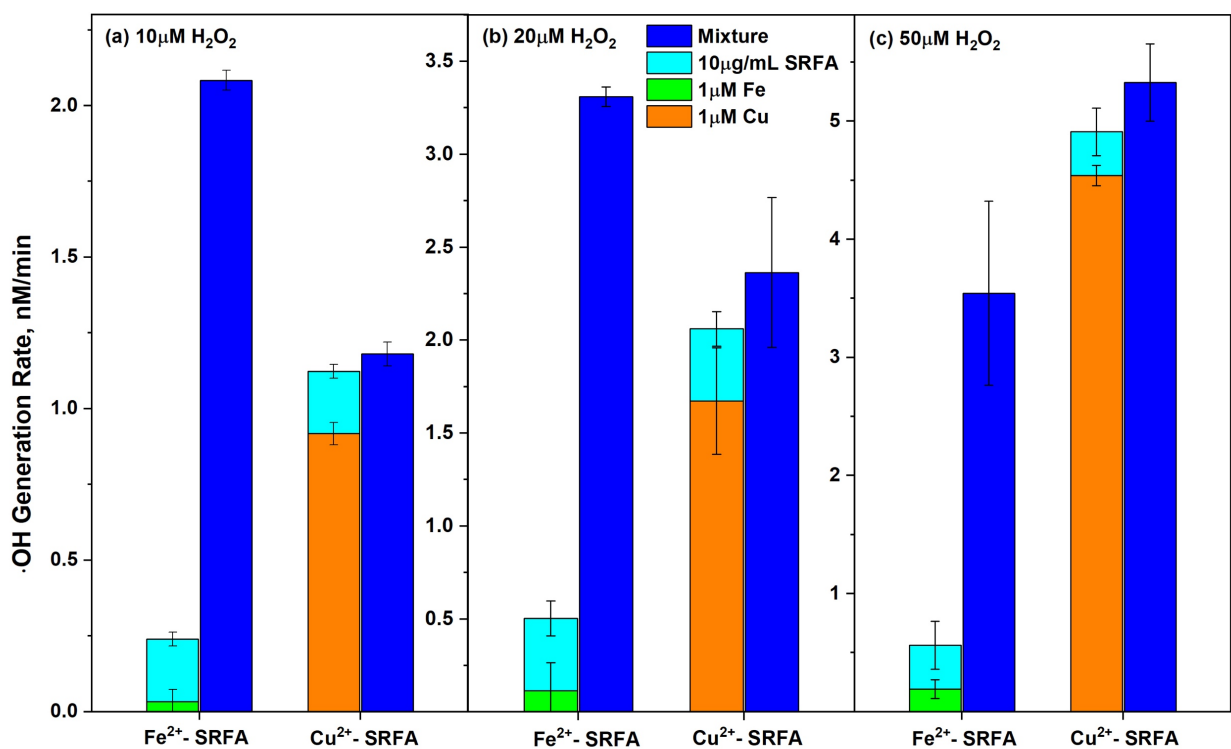


Figure 8. Rate of ·OH generation from 10 μM, 20 μM and 50 μM H₂O₂ by the mixture of SRFA with Fe/Cu and their individual compounds

The ·OH generation in Fenton-like reaction is initiated by Cu(I). However, due to its relative abundance in the ambient PM, and the dominant contribution to oxidative potential from Cu(II),¹⁷ Cu(II) is of greater concern to assess copper's toxicity. Therefore, we chose Cu(II) to assess the Cu-H₂O₂ reaction. An alternative mechanism has been suggested in previous studies to account for the capability of Cu(II) to catalyze ·OH production in the Cu-H₂O₂ system.⁷⁰⁻⁷²



Briefly, Cu(II) could oxidize H₂O₂ generating HO₂·, which could in turn reduce Cu(II). The Cu(I) produced in R1 and R2 would then catalyze Fenton-like reaction to generate ·OH, and would be cycled back to Cu(II). Despite the relatively high efficiency for reducing H₂O₂, Cu appears to have

additive effect with SRFA in Fenton-like reaction. Whereas the net result – the $\cdot\text{OH}$ generation in the presence of antioxidants also indicates additive effect of Cu-SRFA, the suppression of Cu-SRFA complexes on the consumption of antioxidants provides important evidence of the alteration for oxidative potential induced by organic complexation of Cu(II).

CHAPTER 4: CONCLUSION

Our results highlight the extent of organic complexation of Fe and Cu in ambient PM, which is rarely investigated in previous studies. Also, the metal-organic ligands are shown to significantly alter the oxidative potential of Fe and Cu from different endpoints, including the generation of hydroxyl radical, consumption of antioxidants, and the capability of converting H_2O_2 to $\cdot\text{OH}$. We developed a novel C-18 fractionation scheme, which quantifies Fe and Cu in different fractions, based on the hydrophobicity of their complexing agents. Generally, over 70-80% of ambient Fe and Cu are found in organic complexes, while hydrophilic metals (50-60%) dominate over hydrophobic metals (20-30%). Among different PM samples, the larger concentration of PM-borne metals detected in hydrophobic fraction, is found to be associated with a higher tendency of being soluble in methanol. Selected as a surrogate of water-soluble atmospheric HULIS, SRFA is shown to effectively chelate Fe and Cu by our scheme. Consistent in different antioxidants systems (SLF and DTT), Fe-SRFA complexes show strongly synergistic effect in generating $\cdot\text{OH}$, while Cu and SRFA are additive. However, the result in AO consumption indicates that Cu-SRFA complexes significantly suppress the destruction of antioxidants, while Fe, SRFA and Fe-SRFA complexes are sufficiently inactive, thus inadequate to account for the synergy in the production of $\cdot\text{OH}$. Instead, the Fenton reaction, whose activity is positively altered by the formation of Fe-SRFA complexes, serves as the driving process responsible for the enhanced $\cdot\text{OH}$ generation in the antioxidants systems. Compared to free Fe, the chelation of Fe and SRFA essentially facilitates the conversion from H_2O_2 to $\cdot\text{OH}$, and overall $\cdot\text{OH}$ formation as a result. Considering the massive proportion of metals (primarily Fe and Cu) complexed with organic compounds in the ambient PM, this finding could be of great importance to elucidate the mechanisms of metal-induced oxidative potential under physiological condition.

REFERENCES

- (1) Katsouyanni, K.; Touloumi, G.; Spix, C.; Schwartz, J.; Balducci, F.; Medina, S.; Rossi, G.; Wojtyniak, B.; Sunyer, J.; Bacharova, L.; et al. Short Term Effects of Ambient Sulphur Dioxide and Particulate Matter on Mortality in 12 European Cities: Results from Time Series Data from the APHEA Project. *Bmj* **1997**, *314* (7095), 1658–1658.
- (2) Pope, C. A. Cardiovascular Mortality and Long-Term Exposure to Particulate Air Pollution: Epidemiological Evidence of General Pathophysiological Pathways of Disease. *Circulation* **2003**, *109* (1), 71–77.
- (3) Schwarze, P. E.; Øvrevik, J.; Låg, M.; Refsnes, M.; Nafstad, P.; Hetland, R. B.; Dybing, E. Particulate Matter Properties and Health Effects: Consistency of Epidemiological and Toxicological Studies. *Human and Experimental Toxicology* **2006**, *25* (10), 559–579.
- (4) Künzli, N.; Mudway, I. S.; Götschi, T.; Shi, T.; Kelly, F. J.; Cook, S.; Burney, P.; Forsberg, B.; Gauderman, J. W.; Hazenkamp, M. E.; et al. Comparison of Oxidative Properties, Light Absorbance, and Total and Elemental Mass Concentration of Ambient PM_{2.5} collected at 20 European Sites. *Environmental Health Perspectives* **2006**, *114* (5), 684–690.
- (5) Kulshrestha, A.; Satsangi, P. G.; Masih, J.; Taneja, A. Metal Concentration of PM_{2.5} and PM₁₀ Particles and Seasonal Variations in Urban and Rural Environment of Agra, India. *Science of The Total Environment* **2009**, *407* (24), 6196–6204.
- (6) Chen, L. C.; Lippmann, M. *Effects of Metals within Ambient Air Particulate Matter (PM) on Human Health*; 2009.
- (7) Schaumann, F.; Borm, P. J. A.; Herbrich, A.; Knoch, J.; Pitz, M.; Schins, R. P. F.; Luettig, B.; Hohlfeld, J. M.; Heinrich, J.; Krug, N. Metal-Rich Ambient Particles (Particulate

- Matter2.5) Cause Airway Inflammation in Healthy Subjects. *American Journal of Respiratory and Critical Care Medicine* **2004**, *170* (8), 898–903.
- (8) Costa, D. L.; Dreher, K. L.; Costa, D. L.; Dreher, K. L. Bioavailable Transition Metals in Particulate Matter Mediate Cardiopulmonary Injury in Healthy and Compromised Animal Models Published by : The National Institute of Environmental Health Sciences Stable URL : [Http://Www.Jstor.Org/Stable/3433509](http://www.jstor.org/stable/3433509) Linked Ref. **2017**, *105*, 1053–1060.
- (9) Chapman, R. S.; Watkinson, W. P.; Dreher, K. L.; Costa, D. L. Ambient Particulate Matter and Respiratory and Cardiovascular Illness in Adults: Particle-Borne Transition Metals and the Heart-Lung Axis. *Environmental Toxicology and Pharmacology* **1997**, *4* (3–4), 331–338.
- (10) Araujo, J. A.; Nel, A. E. Particulate Matter and Atherosclerosis: Role of Particle Size, Composition and Oxidative Stress. *Particle and Fibre Toxicology* **2009**, *6* (1), 1–19.
- (11) Steenhof, M.; Gosens, I.; Strak, M.; Godri, K. J.; Hoek, G.; Cassee, F. R.; Mudway, I. S.; Kelly, F. J.; Harrison, R. M.; Lebret, E.; et al. In Vitro Toxicity of Particulate Matter (PM) Collected at Different Sites in the Netherlands Is Associated with PM Composition, Size Fraction and Oxidative Potential - the RAPTES Project. *Particle and Fibre Toxicology* **2011**, *8*, 1–15.
- (12) Ayres, J. G.; Borm, P.; Cassee, F. R.; Castranova, V.; Donaldson, K.; Ghio, A.; Harrison, R. M.; Hider, R.; Kelly, F.; Kooter, I. M.; et al. Evaluating the Toxicity of Airborne Particulate Matter and Nanoparticles by Measuring Oxidative Stress Potential - A Workshop Report and Consensus Statement. *Inhalation Toxicology* **2008**, *20* (1), 75–99.

- (13) See, S. W.; Wang, Y. H.; Balasubramanian, R. Contrasting Reactive Oxygen Species and Transition Metal Concentrations in Combustion Aerosols. *Environmental Research* **2007**, *103* (3), 317–324.
- (14) Distefano, E.; Eiguren-Fernandez, A.; Delfino, R. J.; Sioutas, C.; Froines, J. R.; Cho, A. K. Determination of Metal-Based Hydroxyl Radical Generating Capacity of Ambient and Diesel Exhaust Particles. *Inhalation Toxicology* **2009**, *21* (9), 731–738.
- (15) Vidrio, E.; Jung, H.; Anastasio, C. Generation of Hydroxyl Radicals from Dissolved Transition Metals in Surrogate Lung Fluid Solutions. *Atmospheric Environment* **2008**, *42* (18), 4369–4379.
- (16) Xiong, Q.; Yu, H.; Wang, R.; Wei, J.; Verma, V. Rethinking The Dithiothreitol (DTT) Based PM Oxidative Potential: Measuring DTT Consumption versus ROS Generation. *Environmental Science & Technology* **2017**, acs.est.7b01272.
- (17) Charrier, J. G.; Anastasio, C. On Dithiothreitol (DTT) as a Measure of Oxidative Potential for Ambient Particles: Evidence for the Importance of Soluble Transition Metals. **2013**, *31* (9), 1713–1723.
- (18) Kieber, R. J.; Williams, K.; Willey, J. D.; Skrabal, S.; Jr, G. B. A. Iron Speciation in Coastal Rainwater : Concentration and Deposition to Seawater. **2001**.
- (19) Paris, R.; Desboeufs, K. V.; Journet, E. Variability of Dust Iron Solubility in Atmospheric Waters: Investigation of the Role of Oxalate Organic Complexation. *Atmospheric Environment* **2011**, *45* (36), 6510–6517.
- (20) Kieber, R. J.; Skrabal, S. A.; Smith, B. J.; Willey, J. D. Organic Complexation of Fe(II) and Its Impact on the Redox Cycling of Iron in Rain. *Environmental Science and Technology* **2005**, *39* (6), 1576–1583.

- (21) Deguillaume, L.; Leriche, M.; Desboeufs, K.; Mailhot, G.; George, C.; Chaumerliac, N. Transition Metals in Atmospheric Liquid Phases: Sources, Reactivity, and Sensitive Parameters. *Chemical Reviews*. 2005, pp 3388–3431.
- (22) Paris, R.; Desboeufs, K. V. Effect of Atmospheric Organic Complexation on Iron-Bearing Dust Solubility. *Atmospheric Chemistry and Physics* **2013**, *13* (9), 4895–4905.
- (23) Scheinhardt, S.; Müller, K.; Spindler, G.; Herrmann, H. Complexation of Trace Metals in Size-Segregated Aerosol Particles at Nine Sites in Germany. *Atmospheric Environment* **2013**, *74*, 102–109.
- (24) Witt, M.; Jickells, T. Copper Complexation in Marine and Terrestrial Rain Water. *Atmospheric Environment* **2005**, *39* (40), 7657–7666.
- (25) Sunda, W. G.; Lewis, J. A. M. Effect of Complexation by Natural Organic Ligands on the Toxicity of Copper to a Unicellular Alga, *Monochrysis Lutheri*. *Limnology and Oceanography* **1978**, *23* (5), 870–876.
- (26) Spokes, L. J.; Campos, M. L. A. M.; Jickells, T. D. The Role of Organic Matter in Controlling Copper Speciation in Precipitation. *Atmospheric Environment* **1996**, *30* (23), 3959–3966.
- (27) Kabra, K.; Chaudhary, R.; Sawhney, R. L. Solar Photocatalytic Removal of Cu(II), Ni(II), Zn(II) and Pb(II): Speciation Modeling of Metal-Citric Acid Complexes. *Journal of Hazardous Materials* **2008**, *155* (3), 424–432.
- (28) Hartland, A.; Fairchild, I. J.; Lead, J. R.; Zhang, H.; Baalousha, M. Size, Speciation and Lability of NOM-Metal Complexes in Hyperalkaline Cave Dripwater. *Geochimica et Cosmochimica Acta* **2011**, *75* (23), 7533–7551.

- (29) Pérez-Esteban, J.; Escolástico, C.; Moliner, A.; Masaguer, A. Chemical Speciation and Mobilization of Copper and Zinc in Naturally Contaminated Mine Soils with Citric and Tartaric Acids. *Chemosphere* **2013**, *90* (2), 276–283.
- (30) Fuzzi, S.; Andreae, M. O.; Huebert, B. J.; Kulmala, M.; Bond, T. C.; Boy, M.; Doherty, S. J.; Guenther, A.; Kanakidou, M.; Kawamura, K.; et al. Critical Assessment of the Current State of Scientific Knowledge, Terminology, and Research Needs Concerning the Role of Organic Aerosols in the Atmosphere, Climate, and Global Change. *Atmospheric Chemistry and Physics Discussions* **2005**, *5* (6), 11729–11780.
- (31) Laskin, J.; Laskin, A.; Roach, P. J.; Slysz, G. W.; Anderson, G. A.; Nizkorodov, S. A.; Bones, D. L.; Nguyen, L. Q. High-Resolution Desorption Electrospray Ionization Mass Spectrometry for Chemical Characterization of Organic Aerosols. *Analytical Chemistry* **2010**, *82* (5), 2048–2058.
- (32) Emmenegger, L.; Whitney King, D.; Sigg, L.; Sulzberger, B. Oxidation Kinetics of Fe(II) in a Eutrophic Swiss Lake. *Environmental Science and Technology* **1998**, *32* (19), 2990–2996.
- (33) Pullin, M. J.; Cabaniss, S. E. The Effects of PH, Ionic Strength, and Iron-Fulvic Acid Interactions on the Kinetics of Non-Photochemical Iron Transformations. I. Iron(II) Oxidation and Iron(III) Colloid Formation. *Geochimica et Cosmochimica Acta* **2003**, *67* (21), 4067–4077.
- (34) Win, M. S.; Tian, Z.; Zhao, H.; Xiao, K.; Peng, J.; Shang, Y.; Wu, M.; Xiu, G.; Lu, S.; Yonemochi, S.; et al. Atmospheric HULIS and Its Ability to Mediate the Reactive Oxygen Species (ROS): A Review. *Journal of Environmental Sciences* **2017**, *4*, 1–19.

- (35) Okochi, H.; Brimblecombe, P. Potential Trace Metal-Organic Complexation in the Atmosphere. *TheScientificWorldJournal* **2002**, *2*, 767–786.
- (36) Arakaki, T.; Saito, K.; Okada, K.; Nakajima, H.; Hitomi, Y. Contribution of Fulvic Acid to the Photochemical Formation of Fe(II) in Acidic Suwannee River Fulvic Acid Solutions. *Chemosphere* **2010**, *78* (8), 1023–1027.
- (37) Charrier, J. G.; Anastasio, C. Rates of Hydroxyl Radical Production from Transition Metals and Quinones in a Surrogate Lung Fluid. *Environmental Science and Technology* **2015**, *49* (15), 9317–9325.
- (38) Miller, C. J.; Rose, A. L.; Waite, T. D. Hydroxyl Radical Production by H₂O₂-Mediated Oxidation of Fe(II) Complexed by Suwannee River Fulvic Acid under Circumneutral Freshwater Conditions. *Environmental Science and Technology* **2013**, *47* (2), 829–835.
- (39) Voelker, B. M.; Sulzberger, B. Effects of Fulvic Acid on Fe(II) Oxidation by Hydrogen Peroxide. *Environmental Science and Technology* **1996**, *30* (4), 1106–1114.
- (40) Baduel, C.; Voisin, D.; Jaffrezo, J. L. Comparison of Analytical Methods for Humic Like Substances (HULIS) Measurements in Atmospheric Particles. **2009**, 5949–5962.
- (41) Hatch, C. D.; Gierlus, K. M.; Schuttlefield, J. D.; Grassian, V. H. Water Adsorption and Cloud Condensation Nuclei Activity of Calcite and Calcite Coated with Model Humic and Fulvic Acids. *Atmospheric Environment* **2008**, *42* (22), 5672–5684.
- (42) Fujii, M.; Rose, A. L.; Waite, T. D.; Omura, T. Oxygen and Superoxide-Mediated Redox Kinetics of Iron Complexed by Humic Substances in Coastal Seawater. *Environmental Science and Technology* **2010**, *44* (24), 9337–9342.

- (43) Gonzalez, D. H.; Cala, C. K.; Peng, Q.; Paulson, S. E. HULIS Enhancement of Hydroxyl Radical Formation from Fe(II): Kinetics of Fulvic Acid-Fe(II) Complexes in the Presence of Lung Antioxidants. *Environmental Science and Technology* **2017**, *51* (13), 7676–7685.
- (44) Yu, H.; Wei, J.; Cheng, Y.; Subedi, K.; Verma, V. Synergistic and Antagonistic Interactions among the Particulate Matter Components in Generating Reactive Oxygen Species Based on the Dithiothreitol Assay. *Environmental Science & Technology* **2018**, acs.est.7b04261.
- (45) Paciolla, M. D.; Kolla, S.; Jansen, S. A. The Reduction of Dissolved Iron Species by Humic Acid and Subsequent Production of Reactive Oxygen Species. *Advances in Environmental Research* **2002**, *7* (1), 169–178.
- (46) Fulda, B.; Voegelin, A.; Maurer, F.; Christl, I.; Kretzschmar, R. Copper Redox Transformation and Complexation by Reduced and Oxidized Soil Humic Acid. 1. X-Ray Absorption Spectroscopy Study. *Environmental Science and Technology* **2013**, *47* (19), 10903–10911.
- (47) Maurer, F.; Christl, I.; Fulda, B.; Voegelin, A.; Kretzschmar, R. Copper Redox Transformation and Complexation by Reduced and Oxidized Soil Humic Acid. 2. Potentiometric Titrations and Dialysis Cell Experiments. *Environmental Science and Technology* **2013**, *47* (19), 10912–10921.
- (48) Varga, B.; Kiss, G.; Ganszky, I.; Gelencsér, a; Krivácsy, Z. Isolation of Water-Soluble Organic Matter from Atmospheric Aerosol. *Talanta* **2001**, *55* (3), 561–572.
- (49) Sullivan, A. P.; Weber, R. J. Chemical Characterization of the Ambient Organic Aerosol Soluble in Water: 2. Isolation of Acid, Neutral, and Basic Fractions by Modified Size-Exclusion Chromatography. *Journal of Geophysical Research Atmospheres* **2006**, *111* (5), 1–19.

- (50) Lin, P.; Yu, J. Z. Generation of Reactive Oxygen Species Mediated by Humic-like Substances in Atmospheric Aerosols. *Environmental Science and Technology* **2011**, *45* (24), 10362–10368.
- (51) Verma, V.; Fang, T.; Xu, L.; Peltier, R. E.; Russell, A. G.; Ng, N. L.; Weber, R. J. Organic Aerosols Associated with the Generation of Reactive Oxygen Species (ROS) by Water-Soluble PM_{2.5}. *Environmental Science & Technology* **2015**, *49* (7), 4646–4656.
- (52) Stookey, L. L. Ferrozine-A New Spectrophotometric Reagent for Iron. *Analytical Chemistry* **1970**, *42* (7), 779–781.
- (53) Majestic, B. J.; Schauer, J. J.; Shafer, M. M.; Turner, J. R.; Fine, P. M.; Singh, M.; Sioutas, C. Development of a Wet-Chemical Method for the Speciation of Iron in Atmospheric Aerosols. *Environmental Science and Technology* **2006**, *40* (7), 2346–2351.
- (54) Moffett, J. W.; Zika, R. G.; Petasne, R. G. Evaluation of Bathocuproine for the Spectrophotometric Determination of Copper(I) in Copper Redox Studies with Applications in Studies of Natural Waters. *Analytica Chimica Acta* **1985**, *175* (C), 171–179.
- (55) Saran, M.; Summer, K. H. Assaying for Hydroxyl Radicals: Hydroxylated Terephthalate Is a Superior Fluorescence Marker than Hydroxylated Benzoate. *Free Radical Research* **1999**, *31* (5), 429–436.
- (56) Kimoto, E.; Terada, S.; Yamaguchi, T. Analyst of Ascorbic Acid, Dehydroascorbic Acid, and Transformation Products by Ion-Pairing High-Performance Liquid Chromatography with Multiwavelength Ultraviolet and Electrochemical Detection. *Methods in Enzymology* **1997**, *279*, 3–12.

- (57) Senft, A. P.; Dalton, T. P.; Shertzer, H. G. Determining Glutathione and Glutathione Disulfide Using the Fluorescence Probe O-Phthalaldehyde. *Analytical Biochemistry* **2000**, *280* (1), 80–86.
- (58) Abcam. GSH, GSSG and Total Glutathione Assay Kit. *Read* **2012**, 94043–94043.
- (59) Urréjola, S.; Sánchez, A.; Hervello, M. F. Solubilities of Sodium, Potassium, and Copper(II) Sulfates in Ethanol-Water Solutions. *Journal of Chemical and Engineering Data* **2011**, *56* (5), 2687–2691.
- (60) Cheng, J.; Chakrabarti, C. L.; Back, M. H.; Schroeder, W. H. Chemical Speciation of Cu, Zn, Pb and Cd in Rain Water. *Analytica Chimica Acta* **1994**, *288* (3), 141–156.
- (61) Nimmo, M.; Fones, G. Application of Adsorptive Cathodic Stripping Voltammetry for the Determination of Cu, Cd, Ni and Co in Atmospheric Samples. *Analytica Chimica Acta* **1994**, *291* (3), 321–328.
- (62) Paris, R.; Desboeufs, K. V. Effect of Atmospheric Organic Complexation on Iron-Bearing Dust Solubility. *Atmospheric Chemistry and Physics* **2013**, *13* (9), 4895–4905.
- (63) Mackey, D. . Cation-Exchange Behaviour of a Range of Adsorbents and Chromatographic Supports with Regard to Their Suitability for Investigating Trace Metal Speciation in Natural Waters. *Journal of Chromatography* **1982**, *242*, 275–287.
- (64) Mackey, D. J. HPLC Analyses of Metal--Organics in Seawater--Interference Effects Attributed to Stationary-Phase Free Silanols. *Marine Chemistry* **1985**, *16*, 105–119.
- (65) Mills, G. L.; Quinn, J. G. Isolation of Dissolved Organic Matter and Copper Organic-Complexes from Estuarine Waters Using Reverse-Phase Liquid Chromatography. *Marine Chemistry* **1981**, *10* (2), 93–102.

- (66) Sunda, W. G.; Hanson, A. K. Measurement of Free Cupric Ion Concentration in Seawater By a Ligand Competition Technique Involving Copper Sorption Onto C-18 SEP-PAK Cartridges. *Limnology and Oceanography* **1987**, *32* (3), 537–551.
- (67) Kachur, A. V; Held, K. D.; Koch, C. J.; Biaglow, J. E.; Kachur, A. V; Koch, C. J.; Biaglow, J. E. Mechanism of Production of Hydroxyl Radicals in the Copper-Catalyzed Oxidation of Dithiothreitol. *Source: Radiation Research* **1997**, *147* (147), 409–415.
- (68) Miller, C. J.; Rose, A. L.; Waite, T. D. Importance of Iron Complexation for Fenton-Mediated Hydroxyl Radical Production at Circumneutral pH. *Frontiers in Marine Science* **2016**, *3*.
- (69) Keenan, C. R.; Sedlak, D. L. Factors Affecting the Yield of Oxidants from the Reaction of Nanonarticulate Zero-Valent Iron and Oxygen. *Environmental Science and Technology* **2008**, *42* (4), 1262–1267.
- (70) Nichela, D. A.; Berkovic, A. M.; Costante, M. R.; Juliarena, M. P.; García Einschlag, F. S. Nitrobenzene Degradation in Fenton-like Systems Using Cu(II) as Catalyst. Comparison between Cu(II)- and Fe(III)-Based Systems. *Chemical Engineering Journal* **2013**, *228*, 1148–1157.
- (71) Millero, F. J.; Sharma, V. K.; Karn, B. The Rate of Reduction of Copper(II) with Hydrogen Peroxide in Seawater. *Marine Chemistry* **1991**, *36* (1–4), 71–83.
- (72) Perez-Benito, J. F. Reaction Pathways in the Decomposition of Hydrogen Peroxide Catalyzed by Copper(II)☆. *Journal of Inorganic Biochemistry* **2004**, *98* (3), 430–438.

APPENDIX A: SUPPLEMENTARY INFORMATION

Table 1. Details of ambient PM sampling in four seasons

Sampling Season	Sample ID	Start Date	End Date	Sampling duration
Spring (March – April)	S1	03/19/2017	03/21/2017	48 hours
	S2	03/21/2017	03/23/2017	
	S3	03/23/2017	03/25/2017	
	S4	03/25/2017	03/27/2017	
	S5	03/27/2017	03/29/2017	
	S6	03/29/2017	03/31/2017	
	S7	03/31/2017	04/02/2017	
	S8	04/03/2017	04/05/2017	
	S9	04/09/2017	04/11/2017	
	S10	04/11/2017	04/13/2017	
Summer (July – August)	S11	07/07/2017	07/10/2017	72 hours
	S12	07/10/2017	07/13/2017	
	S13	07/13/2017	07/16/2017	
	S14	07/17/2017	07/20/2017	
	S15	07/20/2017	07/23/2017	
	S16	07/23/2017	07/26/2017	
	S17	07/27/2017	07/30/2017	
	S18	07/30/2017	08/02/2017	
Fall (October – November)	S19	10/15/2017	10/18/2017	72 hours
	S20	10/18/2017	10/21/2017	
	S21	10/21/2017	10/24/2017	
	S22	10/24/2017	10/27/2017	
	S23	11/01/2017	11/04/2017	
	S24	11/04/2017	11/07/2017	
	S25	11/07/2017	11/10/2017	
Winter (December – February)	S26	12/04/2017	12/07/2017	72 hours
	S27	12/12/2017	12/15/2017	
	S28	02/02/2018	02/05/2018	
	S29	02/13/2018	02/16/2018	
	S30	02/25/2018	02/28/2018	

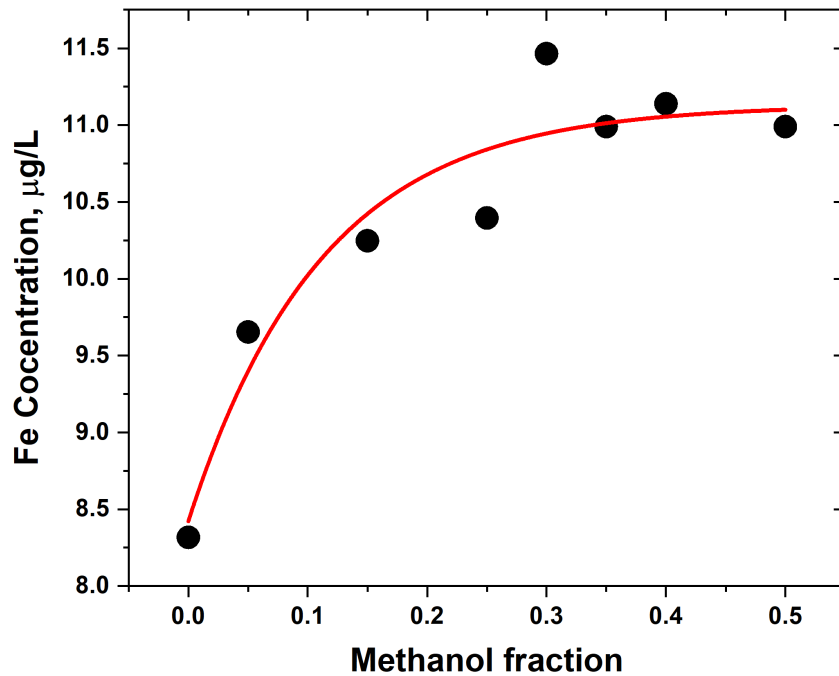


Figure 9. Saturation curve of Fe extraction efficiency of increasing concentrations of methanol solution

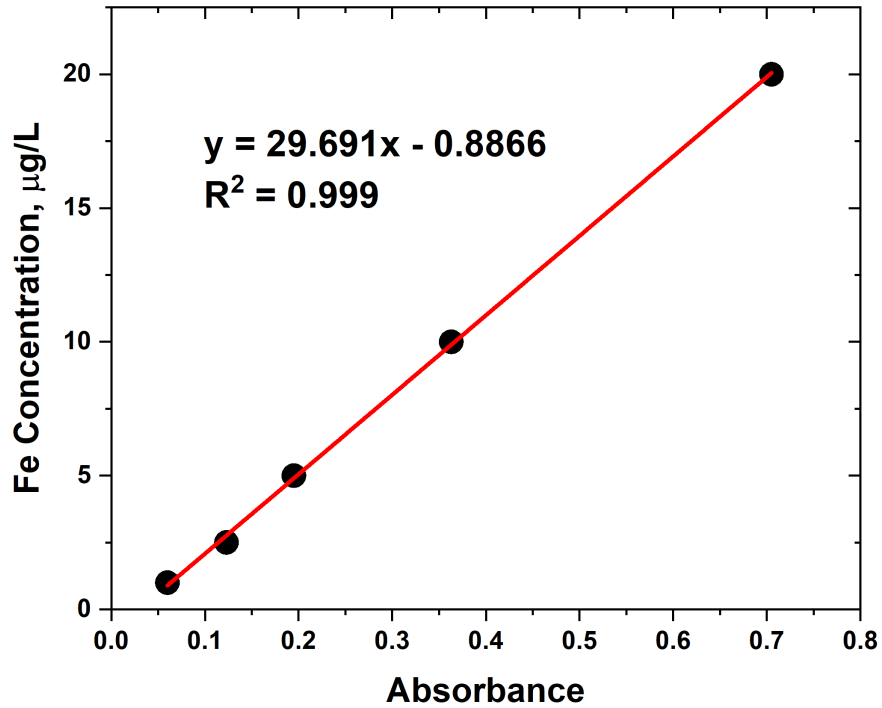


Figure 10. Calibration curve of ferrozine method

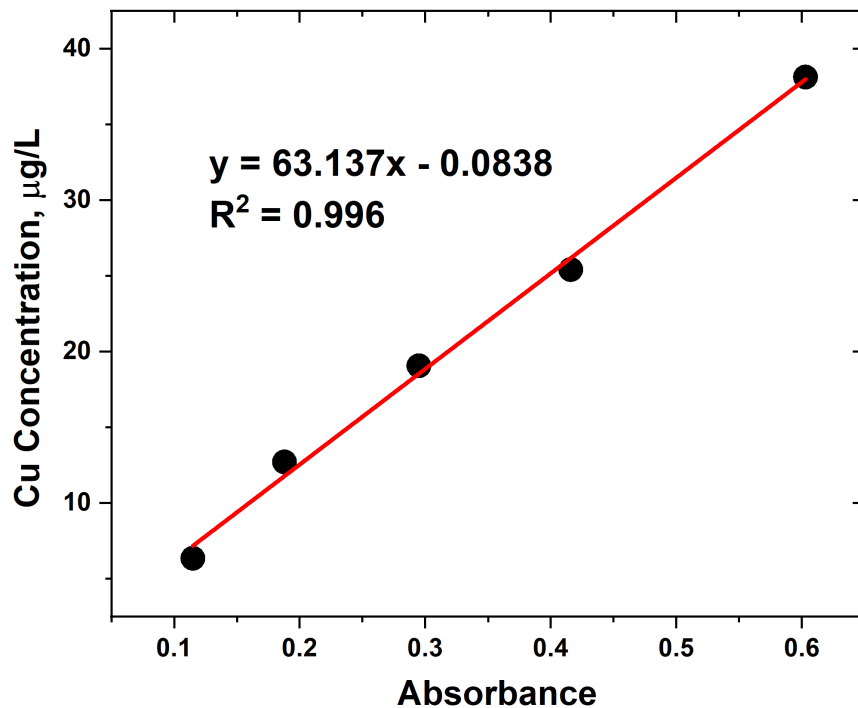


Figure 11. Calibration curve of bathocuproine method

Table 2. AA concentration with different concentrations of Cit, GSH and UA

Measured [AA]/(µM)	Theoretical [AA]/(µM)	Theoretical [Cit]/(µM)	Theoretical [GSH]/(µM)	Theoretical [UA]/(µM)
206.05	200	300	100	100
211.10	200	250	70	70
200.27	200	200	50	50
193.42	200	150	30	30

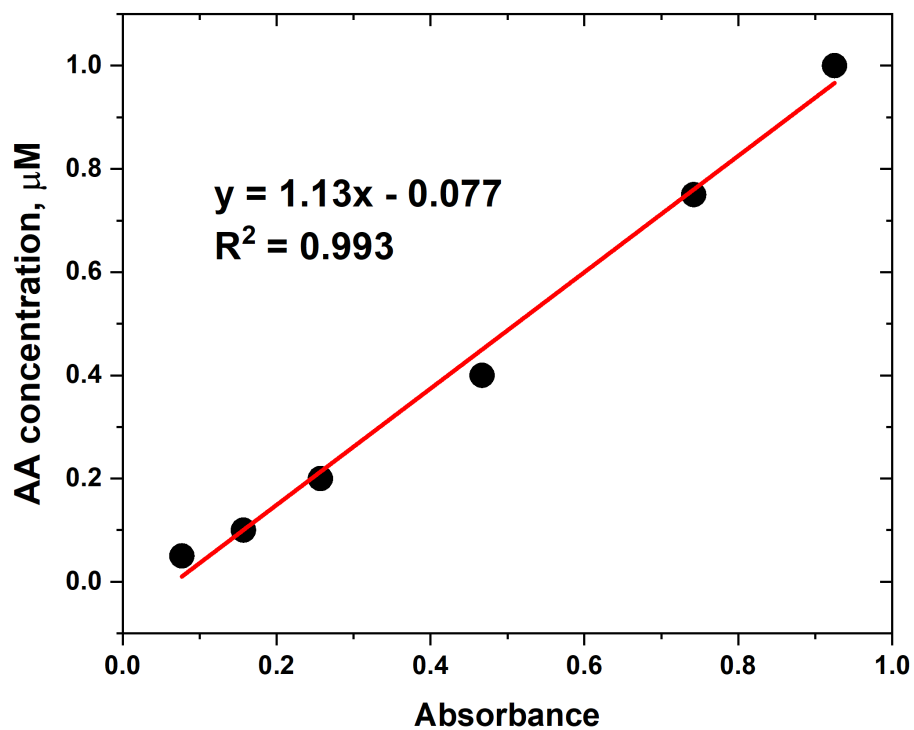


Figure 12. Calibration curve of ascorbic acid (AA) measurement in SLF

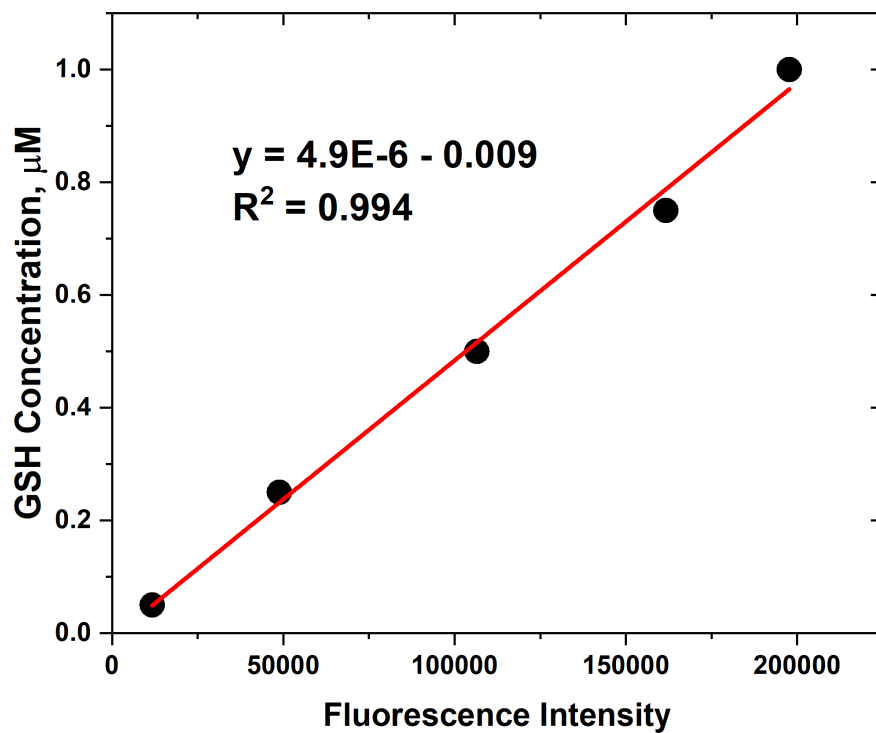


Figure 13. Calibration curve of glutathione (GSH) measurement in SLF